

1 Supplemental Information

2

3	Supplemental Methods	1
4	1. Correlation analysis between gene expression and chromatin accessibility	1
5	2. Downsampling of nuclei	2
6	3. GWAS enrichment analysis	2
7	Supplemental Results	2
8	1. Cell type-specific cis-regulatory gene regulation	2
9	2. Differences in detection power between cell types	3
10	3. GWAS enrichment analysis using H-MAGMA	3
11	Supplemental Figures	4
12		

13 Supplemental Methods

14 1. Correlation analysis between gene expression and chromatin 15 accessibility

16 The assessment of the number of peaks nearby each gene and the number of nearby correlated
17 peaks per gene was performed for each cell type separately on the pseudobulk level. Peaks with
18 less than 5 counts in more than 50% of the samples were removed from the peak matrix and
19 genes with less than 5 counts in more than 75% were excluded from the count matrix. The less
20 stringent filtering in the peaks was applied due to the even sparser signal in ATAC-seq data.
21 Gene expression and peak matrix were normalized with the variance stabilizing transformation
22 in DESeq2⁶⁴. Peaks within a 100 kb window from the gene body, the default distance used to
23 calculate gene scores in ArchR⁴⁷, were considered to be nearby a gene and tested for
24 correlation. Pearson's correlation coefficient was used as a measure of the association between
25 gene expression and chromatin accessibility.

26 In addition to the correlation between gene expression and chromatin accessibility on the peak
27 level, expression levels were also correlated with gene scores. This analysis was performed in
28 each cell type separately and across all cell types. On the pseudobulk level, Pearson's
29 correlation coefficients were calculated across all genes between expression and gene scores
30 averaged across all samples. Additionally, the distribution of Pearson's correlation coefficients
31 calculated between gene expression and gene scores across all pseudobulk samples for each
32 gene was compared to a random distribution obtained by correlating gene expression with a
33 random permutation of gene scores.

34

35 2. Downsampling of nuclei

36 To dissect to what extent the number of DE genes in a cell type is influenced by its nuclei count
37 and consequently the number of genes tested for differential expression, a downsampling
38 analysis was performed. The nuclei per cell type were downsampled to the 75%, 50% and 25%
39 percentiles of nuclei (40,793, 31,504, 14,416 nuclei respectively). Differential expression
40 analysis was performed on the downsampled datasets as described in Methods.
41

42 3. GWAS enrichment analysis

43 GWAS enrichment analysis was performed with H-MAGMA v1.10¹⁰. A mapping of SNPs to
44 genes was generated based on GWAS summary statistics for schizophrenia¹¹, bipolar disorder¹³
45 and MDD¹² and the european 1,000 genomes reference panel downloaded from the H-
46 MAGMA github page (<https://github.com/thewonlab/H-MAGMA>). Based on these results, a
47 gene-level analysis in the form of a gene property analysis was performed with the “--gene-
48 covar” argument in MAGMA. This analysis allows the input of a continuous variable (here:
49 DE (risk) results in the form of $-\log_{10}(\text{p-value}) \cdot \log_2(\text{fold change})$) into the gene-level
50 regression framework to test if DE related to disease status/genetic risk is associated with
51 GWAS results.

52

53 Supplemental Results

54 1. Cell type-specific cis-regulatory gene regulation

55 To elucidate the specific cis-regulatory interactions between chromatin accessibility and gene
56 expression within distinct cell types, independent of any disease phenotype influence, we
57 conducted a thorough analysis. This involved quantifying the number of proximate peaks
58 (within 100 kb of the gene body) for each gene. Subsequently, we correlated the signal of these
59 peaks with gene expression levels after applying appropriate filtering and normalization
60 techniques specific to each cell type.

61 For example, in oligodendrocyte precursor cells (OPCs), the range of nearby peaks within the
62 100 kb region surrounding the gene body ranges from 0 to 112, with a median count of 6. More
63 than 1,500 genes exhibited no proximate peaks in their vicinity (Supp. Figure 2a). While similar
64 patterns emerged for other cell types, they displayed distinct maximum values, consistently
65 low median counts, and a substantial number of genes lacking nearby peaks within the 100 kb
66 region from the gene body. Among the peaks situated near a gene, even fewer demonstrated a
67 significant correlation with the respective gene's expression levels. The maximum number of
68 peaks showing nominal significance ($\text{p-value} \leq 0.05$) was 18, while nearly 8,000 genes were
69 without any correlated peaks (Supp. Figure 2b).

70 Due to this sparse signal on the peak level, we examined the relationship between gene
71 expression and chromatin accessibility on the gene level, making use of gene scores which
72 predict the level of gene expression from the accessibility of gene regulatory elements nearby
73 a gene without the necessity to call peaks. The correlation between the mean normalized gene
74 expression values and gene scores across donors significantly correlates across ($R = 0.47$, Supp.
75 Figure 2c) and within cell types ($R = [0.4, 0.56]$ in all cell types, Supp. Figure 2d). While the
76 correlation between normalized gene expression and gene scores remains high if we correlate
77 the respective pseudobulk samples across all cell types (Supp. Figure 2e), thereby keeping cell
78 type and sample-specific differences in the data, correlations are rather low and partly even
79 negative if we correlate only pseudobulk samples within a specific cell type, thereby keeping
80 only sample-specific differences (Supp. Figure 2f). However, the distribution of correlations is
81 still significantly different from a random distribution, generated with a permutation of the
82 gene scores across pseudobulk samples.

83 As a result, we opted to conduct downstream analyses at the gene score level. This approach
84 addresses the challenge of missing (and correlated) peaks for numerous genes, providing a
85 more comprehensive view of the regulatory landscape surrounding each gene.

86

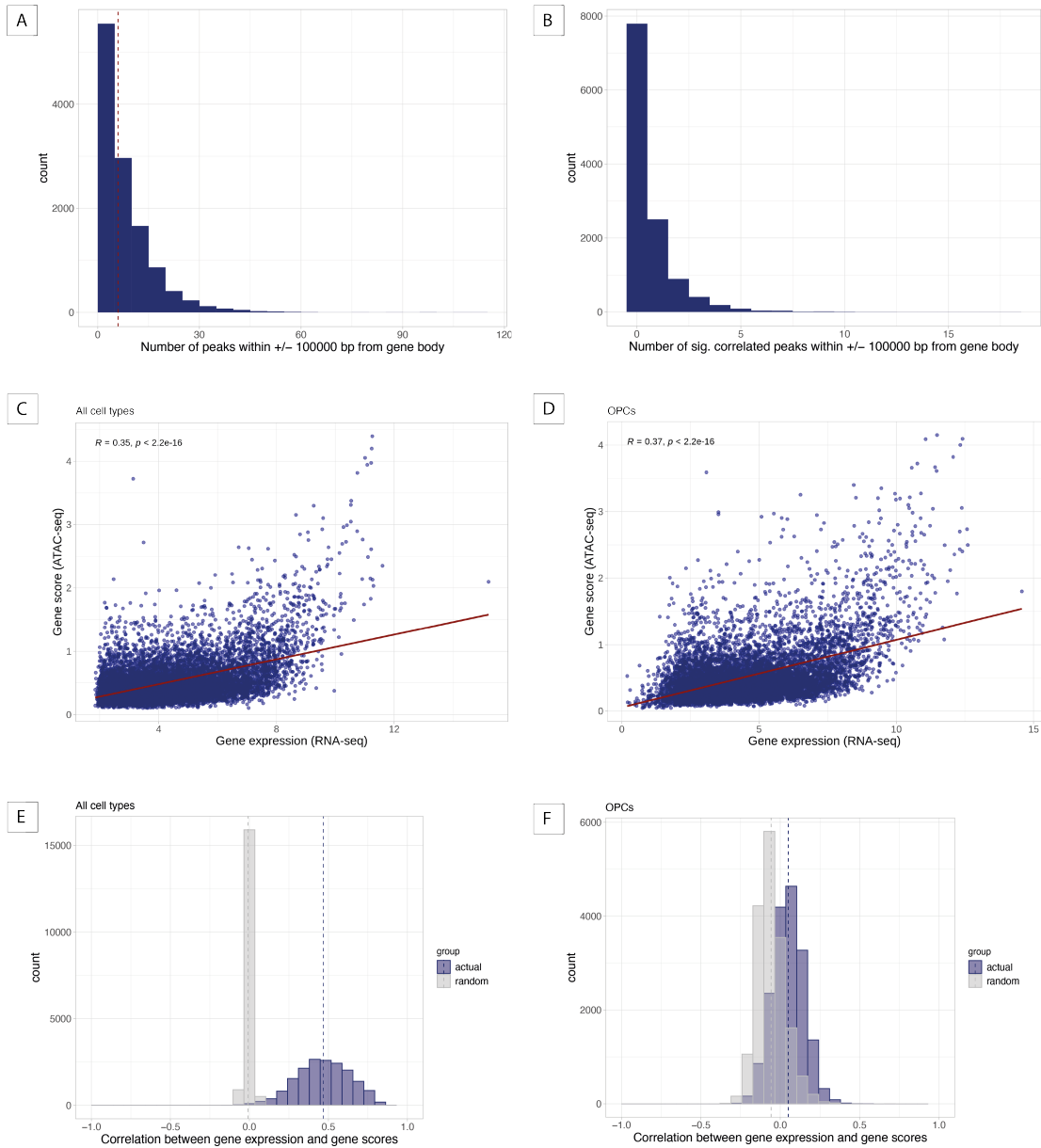
87 2. Differences in detection power between cell types

88 The number of DE genes in each cell type was influenced by its nuclei count (Supp. Figure 3a)
89 and consequently the number of genes tested. Downsampling the nuclei per cell type to the
90 75%, 50% and 25% percentiles of nuclei ($n=40,793, 31,504, 14,416$ respectively), revealed
91 that the gap between the number of tested genes and DE genes in excitatory neurons and other
92 cell types becomes smaller with the level of downsampling, but excitatory neurons still
93 exhibited the highest number of DE genes (Supp. Figure 3b-c).

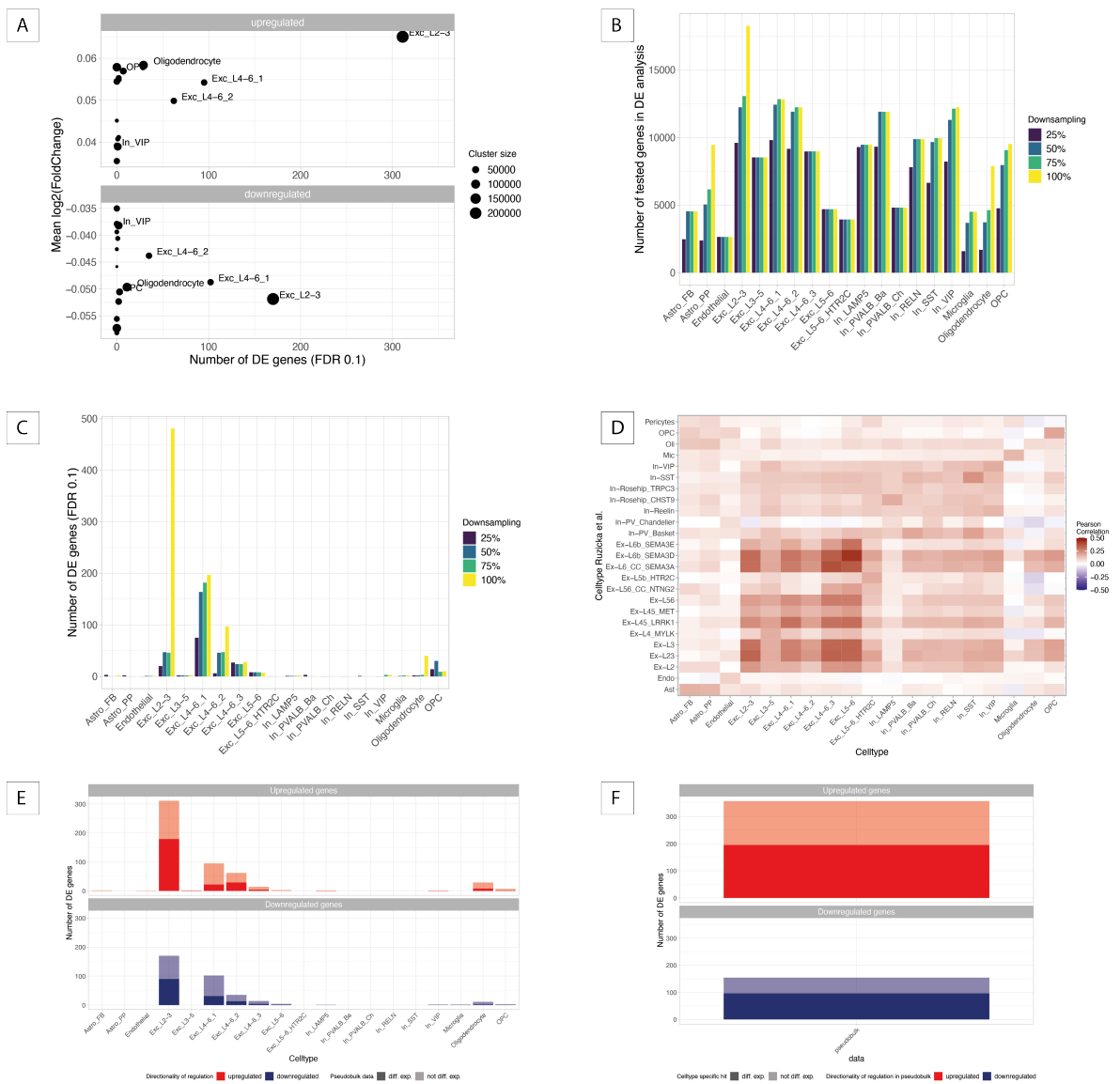
94

95 3. GWAS enrichment analysis using H-MAGMA

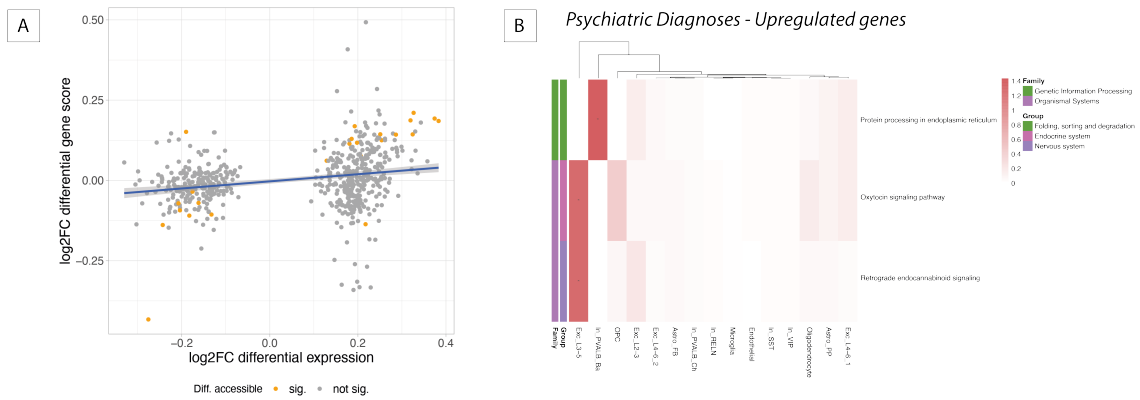
96 To ascertain whether DE risk genes for specific traits and cell types are enriched for GWAS-
97 associated genes for psychiatric disorders (bipolar disorder¹³, MDD¹² and schizophrenia¹¹), we
98 conducted a GWAS enrichment analysis using H-MAGMA¹⁰. No significant enrichments of
99 GWAS-associated genes emerged among the DE risk results for cross-disorder phenotype,
100 bipolar disorder, MDD and height. However, we identified significant enrichments of
101 schizophrenia GWAS-associated genes in the DE risk results for schizophrenia within basket
102 cells (In_PVALB_Ba), excitatory neurons layers 2 to 3 (Exc_L2-3) and endothelial cells
103 (Figure 7b). Similarly, MDD GWAS-associated genes exhibited significant enrichment in
104 endothelial cells' DE risk results for schizophrenia (Figure 7b).



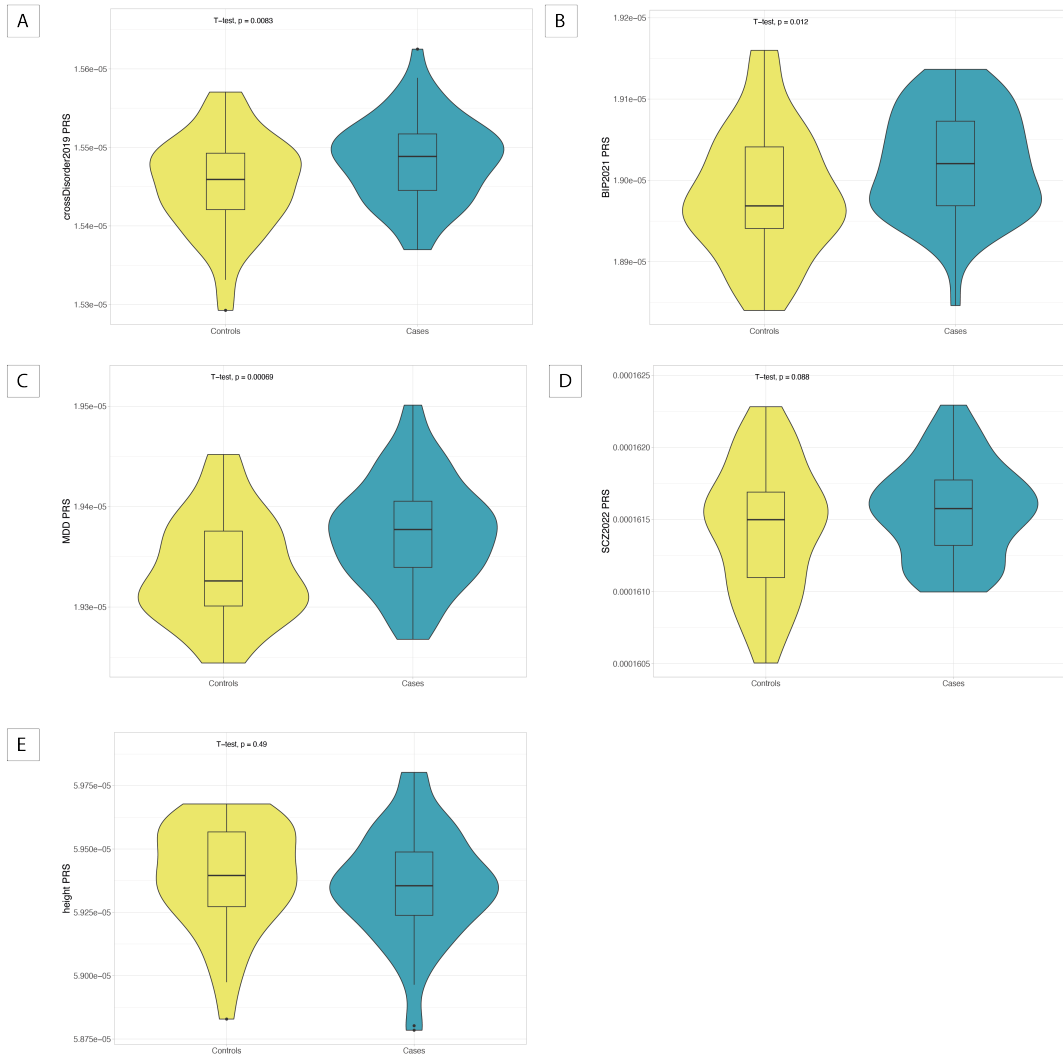
113
 114 **Supp. Figure 2. Cis-regulatory interactions between chromatin accessibility and gene expression.** OPCs
 115 are chosen as an exemplary cell type in this figure. (A) Histogram of the number of peaks within a 100kb
 116 window from the gene body for all genes tested for differential expression in OPCs. Dashed red line indicates
 117 the median number of peaks. (B) Histogram of the number of nominally significantly correlated peaks ($P \leq$
 118 0.05) within a 100kb window from the gene body in OPCs. (C-D) Mean gene expression levels plotted against
 119 mean gene score levels across all cell types (C) and in OPCs (D). The red line represents a linear model fitted on
 120 the data. Pearson correlation is shown in the upper left corner. (E-F) Histogram of correlations between gene
 121 expression and gene score levels on the donor level across all cell types (E) and in OPCs (F). The distribution of
 122 the actual correlation coefficients (blue) is plotted along the distribution obtained by randomly permuting the
 123 donor levels (gray). The dashed line indicates the mean values respectively.



124
 125 **Supp. Figure 3. Transcriptional alterations between psychiatric cases and controls.** (A) Number of DE
 126 genes (FDR ≤ 0.1) plotted against the mean \log_2 -fold change for up- and downregulated genes separately. Dot
 127 size indicates the cluster size. (B-C) Barplot representing the number of genes tested for differential expression
 128 (B) and the number of significant DE genes (C) using the full dataset and datasets downsampled to the 75%,
 129 50% and 25% percentile of nuclei per cell type which is indicated by color. (D) Correlation analysis between
 130 effect sizes from our study and effect sizes reported in Ruzicka et al.²⁶ for each pair of cell types. Color
 131 indicates the Pearson correlation coefficient based on the effect sizes for the shared set of genes tested in the
 132 respective cell types. (E) Barplot representing the number of DE genes per cell type for up- and downregulation
 133 separately and the proportion of genes also identified as DE based on full pseudobulk data, represented by
 134 darker color. (F) Barplot representing the number of DE genes based on full pseudobulk data for up- and
 135 downregulation separately. The darker parts of the bars represent the proportion of genes also identified as DE
 136 in at least one cell type.

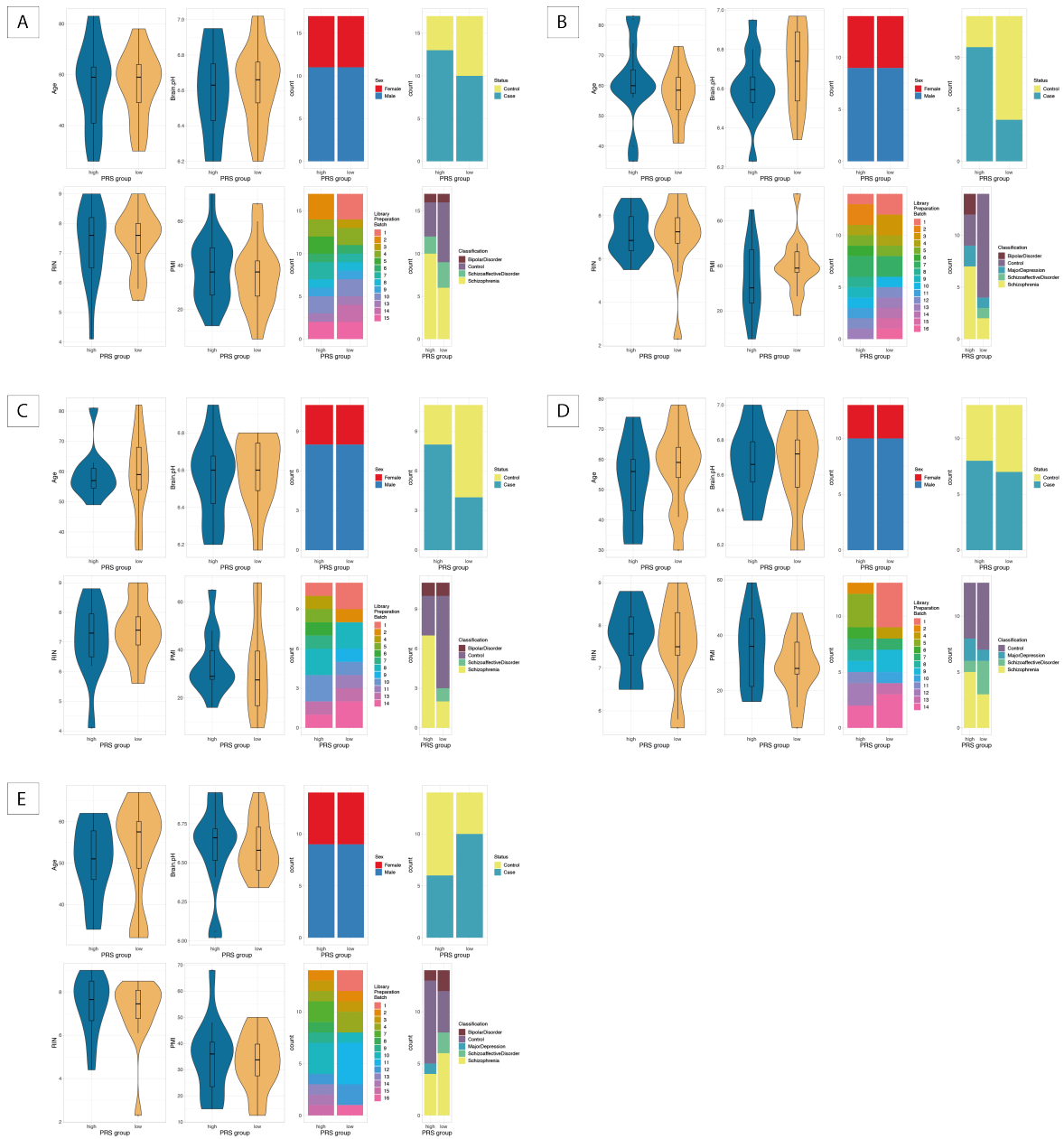


137
 138 **Supp. Figure 4. Epigenomic alterations between psychiatric cases and controls.** (A) Log₂-fold changes of
 139 differential expression and accessibility analysis for all DE genes across cell types plotted against each other
 140 with significance in the same cell type indicated by color. The blue line represents a linear model fitted on the
 141 data. (B) Results of KEGG pathway enrichment analysis for 250 most up- and downregulated genes per cell
 142 type. All pathways significantly enriched in at least one cell type are included into the heatmap. Color represents
 143 $-\log_{10}$ -transformed FDR values and asterisks indicate significance ($FDR \leq 0.05$). Colored annotations of the
 144 pathways on the left side of each plot indicate to which pathway group and family a pathway belongs. The
 145 dendrograms visualize k-means clustering of cell types according to enrichment results.



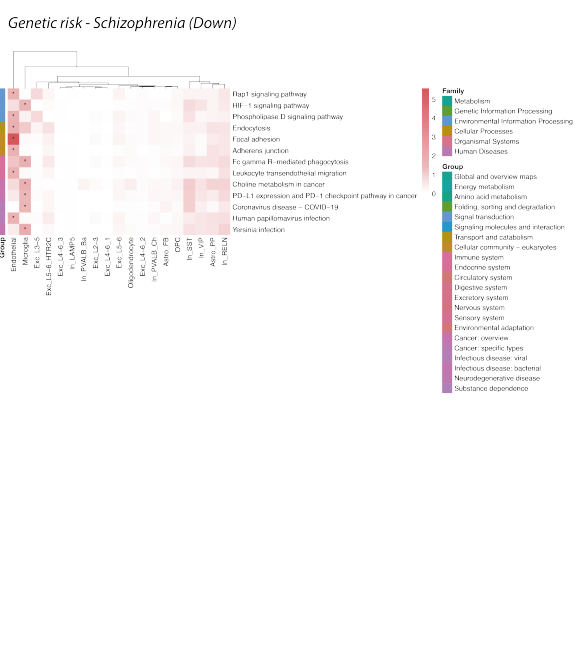
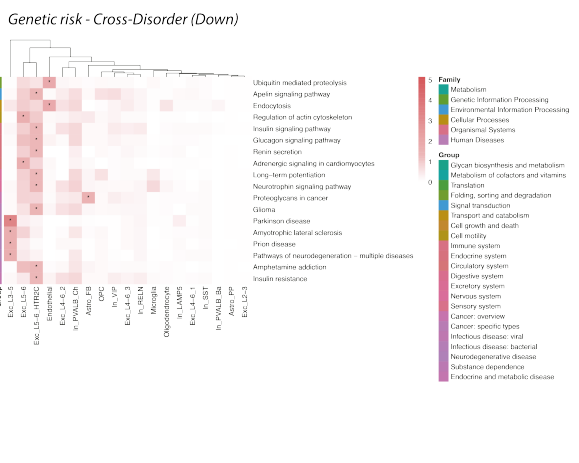
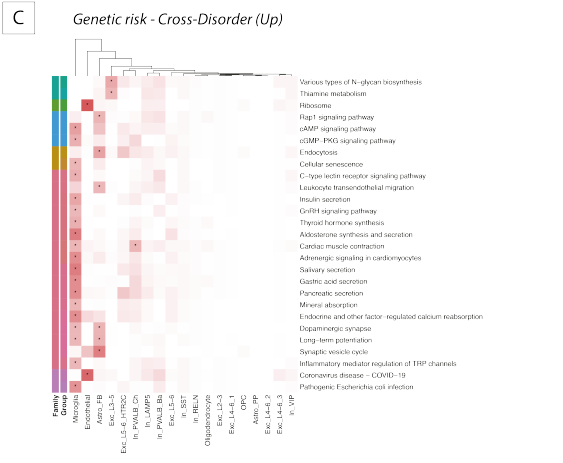
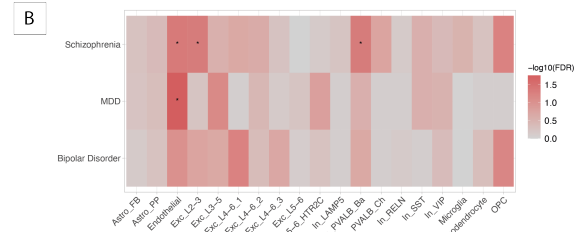
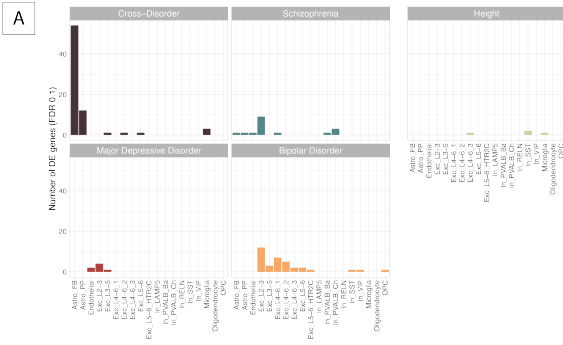
146
147
148
149
150
151

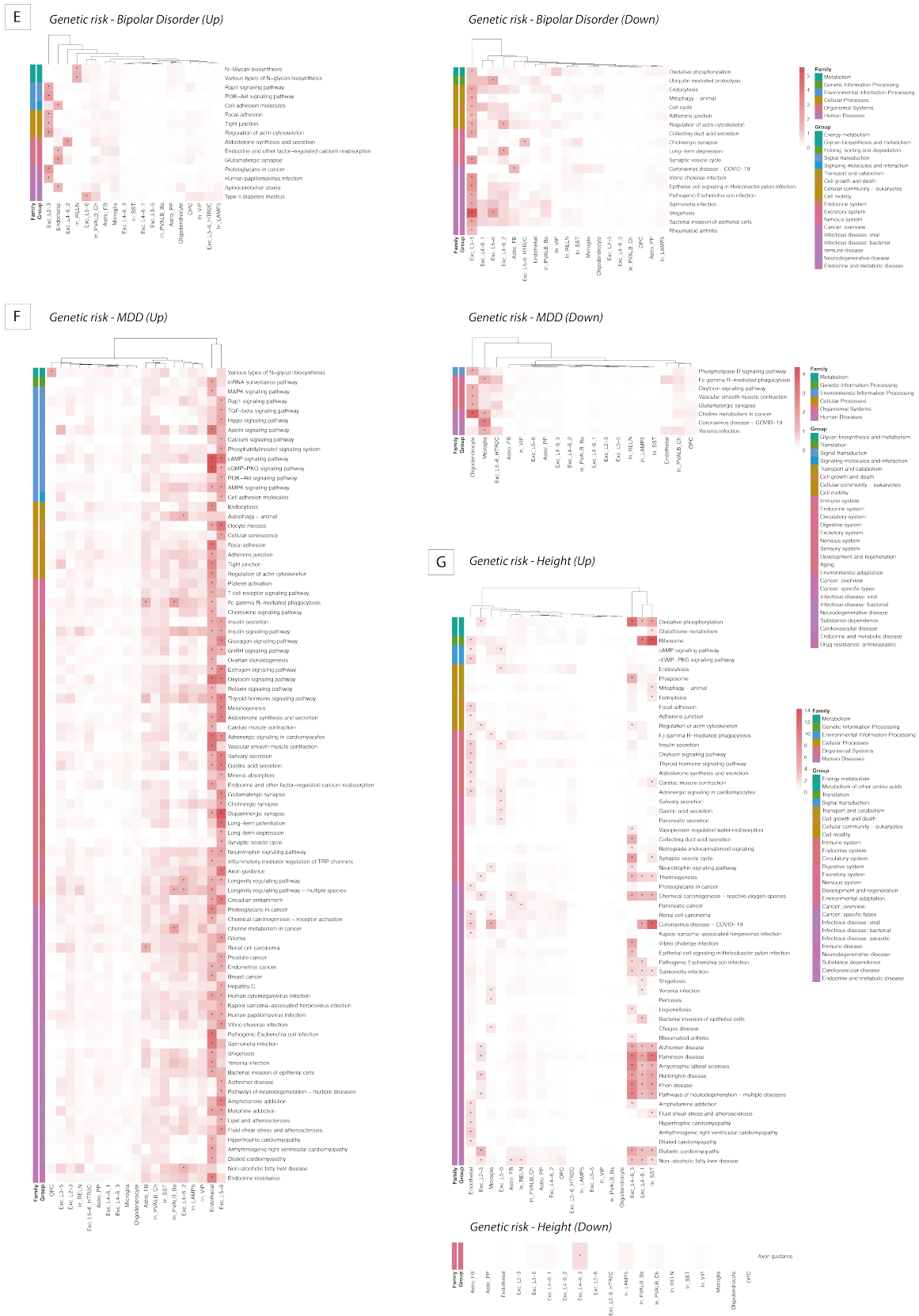
Supp. Figure 5. Genetic risk for psychiatric disorders in cases and controls. (A-E) Distribution of polygenic risk scores (PRS) for cross-disorder phenotype (A), bipolar disorder (B), MDD (C), schizophrenia (D) and height (E) for controls and cases. A one-sided t-test was used to test for differences in cross-disorder, bipolar disorder, MDD and schizophrenia PRS between cases and controls, while a two-sided t-test was used to test for differences in height PRS.



152

153 **Supp. Figure 6. Definition of extreme groups for genetic risk.** (A-E) Matched covariates and distribution of
 154 disease status and diagnoses for high and low risk groups for cross-disorder phenotype (A), bipolar disorder (B),
 155 major depressive disorder (C), schizophrenia (D) and height (E).

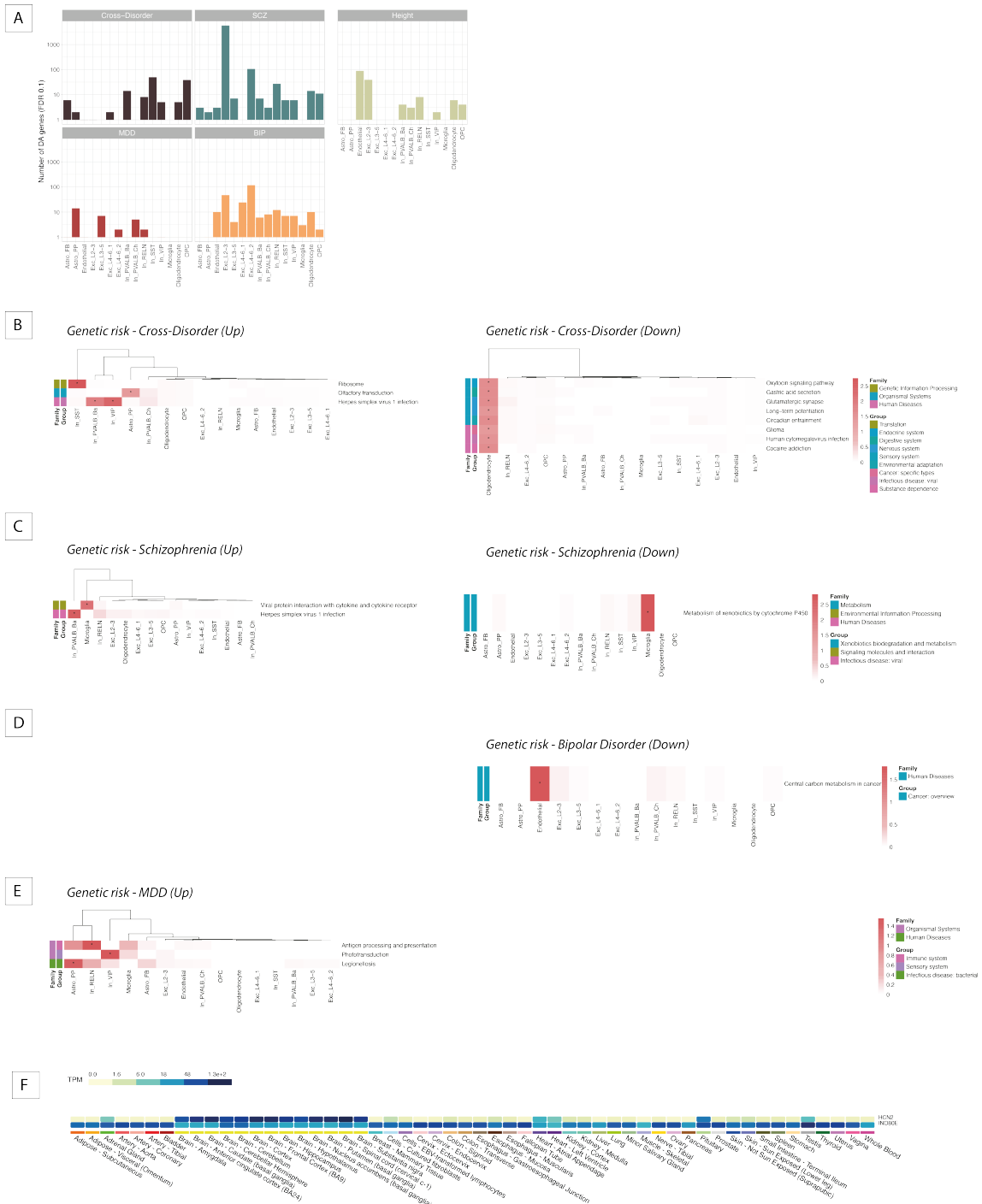




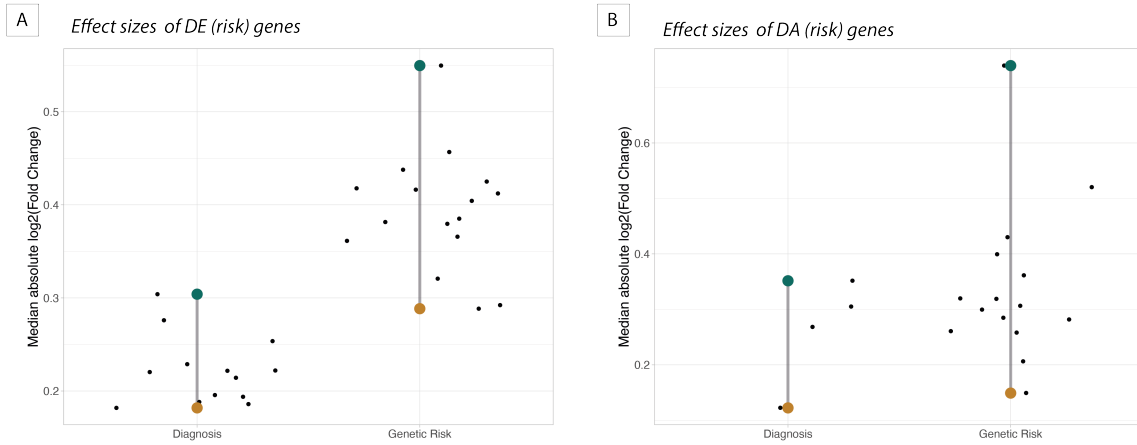
157
158
159
160

Supp. Figure 7. Dysregulations in gene expression between extreme genetic risk groups. (A) Barplot visualizing the number of DE risk genes ($FDR \leq 0.1$) between donors at high and low genetic risk quantified by PRS based on 5 different GWAS studies. **(B)** Results of GWAS enrichment analysis in schizophrenia DE risk

161 genes using H-MAGMA¹¹⁰ for GWAS hits of bipolar disorder, major depressive disorder and schizophrenia.
162 Color indicates $-\log_{10}$ -transformed FDR values and asterisks indicate significance ($FDR \leq 0.05$).
163 (C-G) Results of KEGG pathway enrichment analysis for 250 most up- and downregulated genes per cell type
164 between extreme genetic risk groups for cross-disorder phenotype (C), schizophrenia (D), bipolar disorder (E),
165 MDD (F), and height (G). Left heatmap of each panel shows enrichment results for upregulated genes, while
166 right heatmap of each panel shows results for downregulated genes. All pathways significantly enriched in at
167 least one cell type are included into the heatmap. Color represents $-\log_{10}$ -transformed FDR values and asterisks
168 indicate significance ($FDR \leq 0.05$). Colored annotations of the pathways on the left side of each plot indicate to
169 which pathway group and family a pathway belongs. The dendrograms visualize k-means clustering of cell
170 types according to enrichment results.

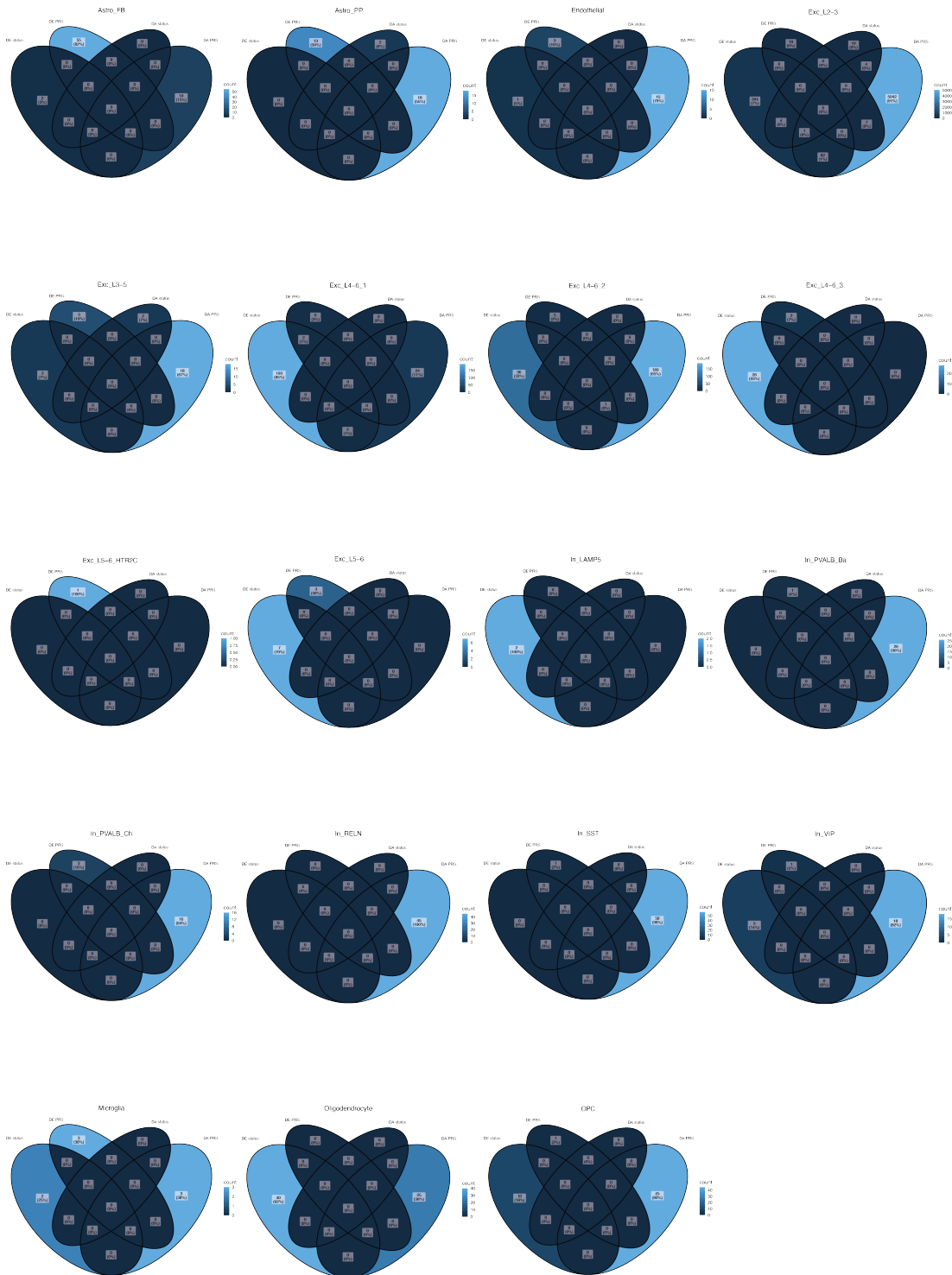


171 **Supp. Figure 8. Dysregulations in chromatin accessibility between extreme genetic risk groups.** (A)
 172 Barplot visualizing the number of DA risk genes (FDR ≤ 0.1) between donors at high and low genetic risk
 173 quantified by PRS based on 5 different GWAS studies. (B-E) Results of KEGG pathway enrichment analysis for
 174 250 most up- and downregulated genes per cell type between extreme genetic risk groups for cross-disorder
 175 phenotype (B), schizophrenia (C), bipolar disorder (D), and MDD (E). No pathways were enriched for height
 176 DA risk genes. Left heatmap of each panel shows enrichment results for upregulated genes, while right heatmap
 177 of each panel shows results for downregulated genes. All pathways significantly enriched in at least one cell
 178 type are included into the heatmap. Color represents $-\log_{10}$ -transformed FDR values and asterisks indicate
 179 significance (FDR ≤ 0.05). Colored annotations of the pathways on the left side of each plot indicate to which
 180 pathway group and family a pathway belongs. The dendrograms visualize k-means clustering of cell types
 181 according to enrichment results. (F) Gene expression levels (i.e. transcript per million, TPM) for *HCN2* and
 182 *INO80E* across multiple human tissues, as sourced from the GTEx portal⁷⁵.



183
184
185
186
187
188

Supp. Figure 9. Range of effect sizes for clinical diagnosis and genetic risk. (A-B) Visualizations of the range of absolute median \log_2 -transformed fold changes per cell type for DE (risk) genes (A) and DA (risk) genes (B). The vertical lines represent the range of effect sizes across cell types with the colored dots representing the minimum and maximum effect size each. Small black dots represent the median effect sizes for specific cell types.



189
190
191
192
193

Supp. Figure 10. Differentially expressed and accessible genes between cases and controls and genetic risk groups. Venn diagram for each cell type comparing DE and DA genes between disease status with DE and DA risk genes between genetic risk groups. DE and DA risk genes are aggregated across the cross-disorder, schizophrenia, MDD and bipolar disorder GWAS studies.